

1 **A GENERALISED RANDOM ENCOUNTER MODEL FOR ESTIMATING**
2 **ANIMAL DENSITY WITH REMOTE SENSOR DATA**

3 **Running title: A generalised random encounter model for animals.**

4 **Word count:**

5 **Authors:**

6 Tim C.D. Lucas^{1,2,3}, Elizabeth A. Moorcroft^{1,4,5}, Robin Freeman⁵, Marcus J. Rowcliffe⁵,
7 Kate E. Jones^{2,5}

8 **Addresses:**

9 1 CoMPLEX, University College London, Physics Building, Gower Street, Lon-
10 don, WC1E 6BT, UK

11 2 Centre for Biodiversity and Environment Research, Department of Genetics,
12 Evolution and Environment, University College London, Gower Street, London,
13 WC1E 6BT, UK

14 3 Department of Statistical Science, University College London, Gower Street,
15 London, WC1E 6BT, UK

16 4 Department of Computer Science, University College London, Gower Street,
17 London, WC1E 6BT, UK

18 5 Institute of Zoology, Zoological Society of London, Regents Park, London, NW1
19 4RY, UK

20 **Corresponding authors:**

21 Kate E. Jones,
22 Centre for Biodiversity and Environment Research,
23 Department of Genetics, Evolution and Environment,
24 University College London,
25 Gower Street,
26 London,
27 WC1E 6BT,
28 UK

29 kate.e.jones@ucl.ac.uk

30

31 Marcus J. Rowcliffe,

32 Institute of Zoology,

33 Zoological Society of London,

34 Regents Park,

35 London,

36 NW1 4RY,

37 UK

38 marcus.rowcliffe@ioz.ac.uk

1. ABSTRACT

1: Wildlife monitoring technology has advanced rapidly and the use of remote sensors such as camera traps, and acoustic detectors is becoming common in both the terrestrial and marine environments. Current capture-recapture or distance methods to estimate abundance or density require individual recognition of animals or knowing the distance of the animal from the sensor, which is often difficult. A method without these requirements, the random encounter model (REM), has been successfully applied to estimate animal densities from count data generated from camera traps. However, count data from acoustic detectors do not fit the assumptions of the REM due to the directionality of animal signals.

2: We developed a generalised REM (gREM), to estimate absolute animal density from count data from both camera traps and acoustic detectors. We derived the gREM for different combinations of sensor detection widths and animal signal widths (a measure of directionality). We tested the accuracy and precision of this model using simulations of different combinations of sensor detection widths and animal signal widths, number of captures, and models of animal movement.

3: We find that the gREM produces accurate estimates of absolute animal density for all combinations of sensor detection widths and animal signal widths. However, larger sensor detection and animal signal widths were found to be more precise. While the model is accurate for all capture efforts tested, the precision of the estimate increases with the number of captures. We found no effect of different animal movement models tested on the accuracy and precision of the gREM.

4: We conclude that the gREM provides an effective method to estimate absolute animal densities from remote sensor count data over a range of sensor and animal signal widths. The gREM is applicable for use for count data obtained in both marine and terrestrial environments, visually or acoustically (e.g., big cats, sharks, birds, bats and cetaceans). As sensors such as camera traps and acoustic detectors become more ubiquitous, the gREM will be increasingly useful for monitoring animal populations across broad spatial, temporal and taxonomic scales.

68 1.1. **Keywords.** Acoustic detection, Camera traps, Marine, Population monitor-
69 ing, Simulations, Terrestrial

70 2. INTRODUCTION

71 Animal population density is one of the fundamental measures needed in ecol-
72 ogy and conservation. The density of a population has important implications
73 for a range of issues such as sensitivity to stochastic fluctuations (??) and risk
74 of extinction (?). Monitoring animal population changes in response to anthro-
75 pogenic pressure is becoming increasingly important as humans modify habi-
76 tats and change climates as never before (?). Sensor technology, such as camera
77 traps (??) and acoustic detectors (???) are becoming increasingly used to monitor
78 changes in animal populations (??), as they are efficient, relatively cheap and non-
79 invasive (?), allowing for surveys over large areas and long periods. However,
80 the problem of converting sampled count data to estimates of density remains as
81 efforts must be made to account for detectability of the animals (?).

82 Methods do already exist for estimating animal density if the distance between
83 the animal and the sensor can be estimated (e.g., capture-mark recapture methods
84 (?) and distance sampling (?)). However, these methods often require additional
85 information that may not be available. For example, capture-mark-recapture meth-
86 ods (????) require recognition of individuals; distance methods require a distance
87 estimation of how far away individuals are from the sensor barlow2005estimates,
88 marques2011estimating. The development of the random encounter model (REM)
89 (a modification of a gas model) enabled animal densities to be estimated from un-
90 marked individuals of a known speed, and sensor detection parameters (?). The
91 REM method has been successfully applied to estimate animal densities from cam-
92 era trap surveys (??). However, extending the REM method to other types of
93 sensors (for example acoustic detectors) is more problematic, because the origi-
94 nal derivation assumes a relatively narrow sensor width (up to $\pi/2$ radians) and
95 that the animal is equally detectable irrespective of its heading (ref).

96 Whilst these restrictions are not problematic for most camera trap makes (e.g.
97 Reconyx, Cuddeback), the REM could not be used to estimate densities from cam-
98 era traps with a wider sensor width (e.g. canopy monitoring with fish eye lens

(?). Additionally, the REM method would not be useful in estimating densities from acoustic survey data as the acoustic detector angles are often wider than $\pi/2$ radians. Acoustic detectors are designed for a range of diverse tasks and environments (?), which will naturally lead to a wide range of sensor detection widths and detection distances. In addition to this, calls emitted by many animals are directional (breaking the assumption of the REM method).

There has been a sharp rise in interest around passive acoustic detectors in recent years, with a 10 fold increase in publications in the decade between 2000 and 2010 (?). Acoustic monitoring is being developed to study many aspects of ecology, including the interactions of animals and their environments (??), the presence and relative abundances of species (?), and biodiversity of an area (?).

Acoustic data suffers from many of the problems associated with data from camera trap surveys in that individuals are often unmarked so capture-make-recapture methods cannot be used to estimate densities. In some cases the distance between the animal and the sensor is known, for example when an array of sensors and the position of the animal is estimated by triangulation (?). In these situations distance-sampling methods can be applied, a method typically used for marine mammals (?). However, in many cases distance estimation is not possible, for example when single sensors are deployed, a situation typical in the majority of terrestrial acoustic surveys (??). In these cases, only relative measures of local abundance can be calculated, and not absolute densities. This means that comparison of populations between species and sites is problematic without assuming equal detectability (?). Equality detectability is unlikely because of differences in environmental conditions, sensor type, habitats, species biology.

In this study we create a generalised REM (gREM), as an extension to the camera trap model of (?), to estimate absolute density from count data from acoustic detectors, or camera traps, where the sensor width can vary from 0 to 2π radians, and the signal given off from the animal can be directional. We assessed the accuracy and precision of the gREM within a simulated environment, by varying the sensor detection widths, animal signal widths, number of captures and models of animal movement. We use the simulation results to recommend best survey practice for estimating animal densities from remote sensors.

3. METHODS

131
132 **3.1. Analytical Model.** The REM presented by (?) adapts the gas model to model
133 count data from camera trap surveys. The REM is derived assuming a stationary
134 sensor with a detection width less than $\pi/2$ radians. However, in order to apply
135 this approach more generally, and in particular to acoustic detectors, we need both
136 to relax the constraint on sensor detection width, and allow for animals with di-
137 rectional signals. Consequently, we derive the gREM for any detection width, θ ,
138 between 0 and 2π with a detection distance r giving a circular sector within which
139 animals can be captured (the detection zone)(Figure 1). Additionally, we model
140 the animal as having an associated signal width α between 0 and 2π (Figure 1, see
141 Appendix S1 for a list of symbols). We start deriving the gREM with the simplest
142 situation, the gas model where $\theta = 2\pi$ and $\alpha = 2\pi$.

143 **3.1.1. Gas Model.** Following ?, we derive the gas model where sensors can capture
144 animals in any direction and animal's signal is detectable from any direction($\theta =$
145 2π and $\alpha = 2\pi$). We assume that animals are in a homogeneous environment,
146 and move in straight lines of random direction with velocity v . We allow that
147 our stationary sensor can capture animals at a detection distance r and that if an
148 animal moves within this detection zone they are captured with a probability of
149 one, while animals outside the zone are never captured.

150 In order to derive animal density, we need to consider relative velocity from
151 the reference frame of the animals. Conceptually, this requires us to imagine that
152 all animals are stationary and randomly distributed in space, while the sensor
153 moves with velocity v . If we calculate the area covered by the sensor during the
154 survey period we can estimate the number of animals the sensor should capture.
155 As a circle moving across a plane, the area covered by the sensor per unit time is
156 $2rv$. The number of expected captures, z , for a survey period of t , with an animal
157 density of D is $z = 2rvtD$. To estimate the density, we rearrange to get $D = z/2rvt$.

158 **3.1.2. gREM derivations for different detection and signal widths.** Different combina-
159 tions of θ and α would be expected to occur (e.g., sensors have different detection
160 widths and animals have different signal widths). For different combinations θ
161 and α , the area covered per unit time is no longer given by $2rv$. Instead of the size

162 of the sensor detection zone having a diameter of $2r$, the size changes with the
 163 approach angle between the sensor and the animal. For any given signal width
 164 and detector width and depending on the angle that the animal approaches the
 165 sensor, the width of the area within which an animal can be detected is called the
 166 profile, p . The size of the profile (averaged across all approach angles) is defined
 167 as the average profile \bar{p} . However, different combinations of θ and α need different
 168 equations to calculate \bar{p} .

169 We have identified the parameter space for the combinations of θ and α for
 170 which the derivation of the equations are the same (defined as sub-models in the
 171 gREM) (Figure 2). For example, the gas model becomes the simplest gREM sub-
 172 model (upper right in (Figure 2) and the REM from (?) is another gREM sub-model
 173 where $\theta < \pi/2$ and $\alpha = 2\pi$. We derive one gREM sub-model SE2 as an example
 174 below (where $4\pi - 2\alpha < \theta < 2\pi$, $0 < \alpha < \pi$) (see Appendix S2 for other gREM
 175 sub-models).

176 3.1.3. *Example derivation of SE2.* In order to calculate \bar{p} , we have to integrate over
 177 the focal angle, x_1 (Figure 3a). This is the angle taken from the centre line of the
 178 sensor. Other focal angles are possible (x_2, x_3, x_4) and are used in other gREM
 179 sub-models (see Appendix S2). As the size of the profile depends on the approach
 180 angle, we present the derivation across all approach angles. When the sensor is
 181 directly approaching the animal $x_1 = \pi/2$.

182 Starting from $x_1 = \pi/2$ until $\theta/2 + \pi/2 - \alpha/2$, the size of the profile is $2r \sin \alpha/2$
 183 (Figure 3b). During this first interval, the size of α limits the width of the profile.
 184 When the animal reaches $x_1 = \theta/2 + \pi/2 - \alpha/2$ (Figure 3c), the size of the profile is
 185 $r \sin(\alpha/2) + r \cos(x_1 - \theta/2)$ and the size of θ and α both limit the width of the profile
 186 (Figure 3c). Finally, at $x_1 = 5\pi/2 - \theta/2 - \alpha/2$ until $x_1 = 3\pi/2$, the width of the profile
 187 is again $2r \sin \alpha/2$ (Figure 3d) and the size of α again limits the width of the profile.

188 The profile width p for π radians of rotation (from directly towards the sensor
 189 to directly behind the sensor) is completely characterised by the three intervals
 190 (Figure 3b–3d). Average profile width \bar{p} is calculated by integrating these profiles
 191 over their appropriate intervals of x_1 and dividing by π which gives

$$\begin{aligned}\bar{p} &= \frac{1}{\pi} \left(\int_{\frac{\pi}{2}}^{\frac{\pi}{2} + \frac{\theta}{2} - \frac{\alpha}{2}} 2r \sin \frac{\alpha}{2} dx_1 + \int_{\frac{\pi}{2} + \frac{\theta}{2} - \frac{\alpha}{2}}^{\frac{5\pi}{2} - \frac{\theta}{2} - \frac{\alpha}{2}} r \sin \frac{\alpha}{2} + r \cos \left(x_1 - \frac{\theta}{2} \right) dx_1 + \int_{\frac{5\pi}{2} - \frac{\theta}{2} - \frac{\alpha}{2}}^{\frac{3\pi}{2}} 2r \sin \frac{\alpha}{2} dx_1 \right) \\ &= \frac{r}{\pi} \left(\theta \sin \frac{\alpha}{2} - \cos \frac{\alpha}{2} + \cos \left(\frac{\alpha}{2} + \theta \right) \right)\end{aligned}\quad \text{eqn 1}$$

We then, as with the gas model, use this expression to calculate density

$$D = z/vt\bar{p} \quad \text{eqn 2}$$

gREM submodels differ discontinuously (figure 2) at different combinations of alpha and theta because the number and nature of intervals needed to describe the average profile width changes. Examine the profile at $x_1 = \theta/2 + \pi/2$ (the profile is perpendicular to the edge of the blind spot.) We see that there is potentially a case where the left side of the profile is $r \sin \alpha/2$ while the right side is zero. This profile does not exist if we return to the full $2r \sin \alpha/2$ profile before $x_1 = \theta/2 + \pi/2$. Therefore we solve $5\pi/2 - \theta/2 - \alpha/2 < \theta/2 + \pi/2$. We find that this new profile only exists if $\alpha < 4\pi - 2\theta$. This inequality defines the line separating models SE2 and its neighbouring model, SE3.

gREM submodel specifications were done by hand, and the integration was done using SymPy (?) in Python (Appendix S3). The gREM submodels were checked by confirming that: 1) submodels adjacent in parameter space were equal at the boundary between them; 2) submodels that border $\alpha = 0$ had $p = 0$ when $\alpha = 0$; 3) average profile widths \bar{p} were between 0 and $2r$ and; 4) each integral, divided by the range of angles that it was integrated over, was between 0 and $2r$. The scripts for these tests are included in Appendix S3 and the R (?) implementation of the gREM is given in Appendix S4.

3.2. Simulation Model. We tested the accuracy and precision of the gREM by developing a spatially explicit simulation of the interaction of sensors and animals using different combinations of sensor detection widths, animal signal widths, number of captures, and models of animal movement. 100 simulations were run where each consisted of a 7.5 km by 7.5 km square (with periodic boundaries). A

stationary sensor of radius r was set up in the exact centre of each simulation, covering 7 sensor detection widths θ between 0 and $2\pi(x, x, x, x, x, x, x)$. Each simulation was populated with a density of 70 animals km^{-2} to match an expected maximum density of mammals in the wild (?). This created a total of 3937 individuals per simulation which were placed randomly at the start of the simulation. Individuals were assigned x signal detection widths α between 0 and $\pi(x, x, x, x, x)$.

The simulation lasted for N steps of duration T during which the individuals moved with a distance d , with an average speed, v . d , was sampled from a normal distribution with mean distance, $\mu_d = vT$, and standard deviation $\sigma_d = vT/10$. An average speed, $v = 40 \text{ km days}^{-1}$, was chosen as this represents the largest day range of terrestrial animals (?), and represents the upper limit of realistic speeds. At the end step, individuals were allowed to either remain stationary for a time step (with a given propability, S), change direction (A) between 0 and π . This resulted in 7 different movement models where: (1) simple movement, where S and $A = 0$; (2) stop-start movement, where (i) $S = 0.25, A = 0$, (ii) $S = 0.5, A = 0$, (iii) $S = 0.75, A = 0$; (3) random walk movement, where (i) $S = 0, A = \pi/3$, (ii) $S = 0, A = 2\pi/3$, (iii) $S = 0, A = \pi$. Individuals were counted as they moved in and out of the detection zone of the sensor.

We calculated the estimated animal density from the gREM by summing the number of captures per simulation and inputting these values into the correct gREM submodel. gREM accuracy was calculated by comparing the density in the simulation with the estimated density. High accuracy is indicated by the mean difference between the estimated and actual values converging to zero as sample size increases.

For each of the 100 simulations we calculate the error (the difference between the known and estimated density) and so we got a distribution of errors which was approximately normal. We constructed boxplots of the estimates error to graphically test for significant differences between the true and estimated densities.

The details of each individual capture event, including the angle between the animals heading and the sensor, were saved from this information the number of capture events can be calculated for a given call angle. The total number of these

247 detections were summed for each set of parameters in the simulation, the gREM
248 was then applied in order to estimate the density in the simulation.

249 The difference between the true input density and density estimated by the
250 gREM were used to

251 Animals were counted as they moved in and out of the detection zone of sta-
252 tionary detectors in the simulation. Multiple detectors were set up in each simula-
253 tion with varying detection angles with the results recorded separately. The details
254 of each individual capture event, including the angle between the animals head-
255 ing and the sensor, were saved from this information the number of capture events
256 can be calculated for a given call angle. The total number of these detections were
257 summed for each set of parameters in the simulation, the gREM was then applied
258 in order to estimate the density in the simulation. The difference between the true
259 input density and density estimated by the gREM were used to evaluate the bias
260 in the analytical models. If the gREM is correct the mean difference between the
261 two values were expected to converge to zero as sample size increases. For each
262 of the 100 simulations we calculate the error (the difference between the known
263 and estimated density) and so we got a distribution of errors which was approxi-
264 mately normal. We constructed boxplots of the estimates error to graphically test
265 for significant differences between the true and estimated densities.

266 All the derived models were tested to demonstrate the accuracy and precision
267 of the gREM while the assumptions of the analytical models were met. We se-
268 lected four example models (models NW1, SW1, NE1, and SE3, as in Figure 2) for
269 demonstrating the accuracy and precision of the gREM with low captures rates,
270 and the accuracy and precision when movement patterns brake the assumptions
271 of the gREM. We specifically looked at a non-continuous movement, and a range
272 of correlated random walks, both of which would be seen in real field conditions.
273 The four models were chosen as they represent one model from each quadrant of
274 Figure 4. The accuracy and precision of all the derived models in the gREM follow
275 the same pattern as the four that have been shown in the main text.

4. RESULTS

276
277 **4.1. Analytical model.** Model results have been derived for each zone with all
278 models except the gas model and REM being newly derived here. However, many
279 models, although derived separately, have the same expression for p . Figure 4
280 shows the expression for p in each case. The general equation for density, using
281 the correct expression for p is then substituted into eqn 2.

282 Although more thorough checks are performed in Appendix S3, it can be seen
283 that all adjacent expressions in Figure 4 are equal when expressions for the bound-
284 aries between them are substituted in.

285 **4.2. Simulation model.** For each model we compared the estimated densities to
286 the true densities in a simulation. None of the models showed any evidence of any
287 significant differences between the estimated and true density values (Figure 5).
288 The precision of the models do vary however. The standard deviation of the error
289 is strongly related to the call and sensor width (Figure 6), such that larger widths
290 have greater precision. However, even the models with small call and sensor an-
291 gles have a relatively high level of precision.

292 The precision of the model is dependent on the number of captures during the
293 survey. In Figure ?? we can see that the model precision gets greater as the num-
294 ber of captures increase. As the number of captures reaches about 100 then the
295 coefficient of variation falls below 10% which could be considered negligible.

296 **4.2.1. Use of the gREM when animal movement is not consistent with model assumptions.**
297 Simulating start-stop instead of continuous movement had no effect the accuracy,
298 or the precision, of the estimates (Figure ??) as long as the true overall speed of
299 the animal is known. Relaxing straight line movement to allow random or cor-
300 related random walks did not effect the accuracy of the method (Figure ??). We
301 allowed animals to change direction up to a maximum value at the end of each
302 step, picked from a uniform distribution where the maximum angle ranged from
303 0 to π , which corresponds to straight line movement and random walk respec-
304 tively. There is no significant difference in the variance for the change, this could
305 be because of the between the step length of the animal movement, 15 minutes,
306 means that immediate double counting of the same animal is unlikely. In the case

307 where large directional changes are likely to occur within short periods of time
308 leading to double counting of the same animal within a short period of time may
309 need to be adjusted because of this.

310 5. DISCUSSION

311 We have developed the gREM such that it can be used to estimate density from
312 acoustic and optical sensors. This has entailed a generalisation of the gas model
313 and the model in (?) to be applicable to any combination of sensor width and call
314 directionality. We have used simulations to show, as a proof of principle, that these
315 models are accurate and precise.

316 The gREM is therefore available for the estimation of density of a number of
317 taxa of importance to conservation, zoonotic diseases and ecosystem services. The
318 models provided are suitable for certain groups for which there are currently no,
319 or few, effective methods for density estimation. Any species that would be consis-
320 tently recorded at least once when within range of a detector would be a suitable
321 subject for the gREM, such as bats (?), songbirds (?), Cetaceans (?) or forest pri-
322 mates (?). Within increasing technological capabilities, this list of species is likely
323 to increase dramatically.

324 Importantly the methods are noninvasive and do not require human marking or
325 naturally identifying marks (as required for mark-recapture models). This makes
326 them suitable for large, continuous monitoring projects with limited human re-
327 sources. It also makes them suitable for species that are under pressure, species
328 that cannot naturally be individually recognised or species that are difficult or
329 dangerous to catch.

330 From our simulations we believe that this method has the potential produce
331 accurate and precise estimates for many different species, using either camera or
332 acoustic detectors. When choosing detectors a researcher should pick the detector
333 with the largest radius and detection angle possible, but whilst a small capture
334 area may reduce precision there is only a limited impact on the overall precision
335 of the model (Figure 6). A range of factors will affect the overall precision of the
336 model, like size of detection zone, speed of animal, density of animals and length
337 of survey which are reflected in the number of captures. Increasing the number of

captures leads to more precise estimates, for species which more slower, or have occur at lower densities, then the detection zone and length of survey need to be increased to compensate so that at least 100 captures are collected (Figure ??).

Within the simulation we have assumed an equal density across the entire world, however in a field environment the situation would be much more complex, with additional variation coming from local changes in density between camera sites. We also assume perfect knowledge of the average speed of an animal and size of the detection zone, and instant triggering of the camera. All of which may lead to possible bias or decreased precision.

Although we have used simulations to validate these models, much more robust testing is needed. Although difficult, proper field test validation would be required before the models could be fully trusted. Note, however, that the REM (?) has been field tested. Both ? and ? both found that the REM were effective manner of estimating animal densities (??). There was some discrepancies between the REM and the census methodologies found by Rovero and Marshall which may have been down to lack of knowledge of wild animal speed, and an underestimate in census results (?). In some taxa gold standard methods of estimating animal density exist, such as capture mark recapture. Where these gold standard exist, and have been proved to work, a simultaneous gREM study could be completed to test the accuracy under field conditions. An easier way to continue to evaluate the models is to run more extensive simulations which break the assumptions of the analytical models. The main element that cannot be analytically treated is the complex movement of real animals. Therefore testing these methods against true animal traces, or more complex movement models would be useful.

There are a number of positive extensions to the gREM which could be developed in the future. The original gas model was formulated for the case where both subjects, either animal and detector, or animal and animal, are moving (?). Indeed any of the models with animals that are equally detectable in all directions ($\alpha = 2\pi$) can be trivially expanded for moving by substituting the sum of the average animal velocity and the sensor velocity for v as used here. However, when the animal has a directional call, the extension becomes much less simple. The

370 approach would be to calculate again the mean profile width. However, for each
371 angle of approach, one would have to average the profile width for an animal fac-
372 ing in any direction (i.e. not necessarily moving towards the sensor) weighted by
373 the relative velocity of that direction. There are a number of situations where a
374 moving detector and animal could occur and as such may be advantage to have
375 a method of estimating densities from the data collected, e.g. an acoustic detector
376 based off a boat when studying Cetacea or sea birds (?).

377 Another interesting, and so far unstudied problem, is edge effects caused by
378 trigger delays (the delay between sensing an animal and attempting to record the
379 encounter) and time expansion acoustic detectors which repeatedly turn on an off
380 during sampling. Both of these have potential biases as animals can move through
381 the detection zone without being detected. The models herein are formulated as-
382 suming constant surveillance and so the error quickly becomes negligible. For ex-
383 ample, if it takes longer for the recording device to be switched on than the length
384 of some animal calls there could be a systematic underestimation of density.

385 6. ACKNOWLEDGMENTS

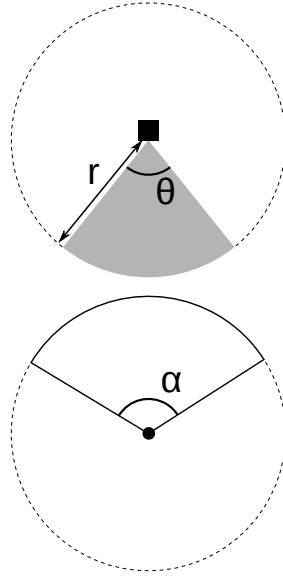


FIGURE 1. Representation of sensor detection width and animal signal width. The filled square and circle represent a sensor and an animal, respectively; θ , sensor detection width (radians); r , sensor detection distance; dark grey shaded area, sensor detection zone; α , animal signal width (radians). Dashed lines around the filled square and circle represents the maximum extent of θ and α , respectively.

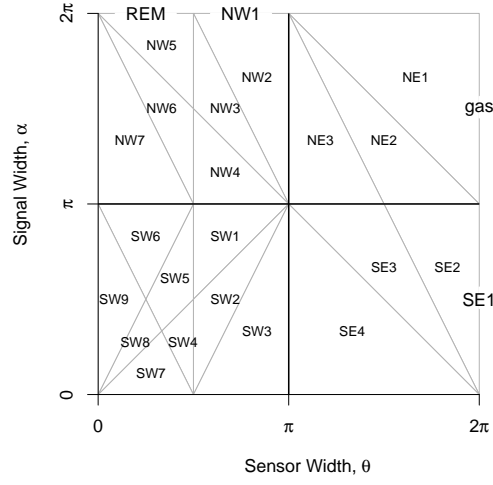


FIGURE 2. Locations where derivation of the average profile \bar{p} is the same for different combinations of sensor detection width and animal signal width. Symbols within each polygon refer to each gREM submodel named after their compass point, except for Gas and REM which highlight the position of these previously derived models within the gREM.

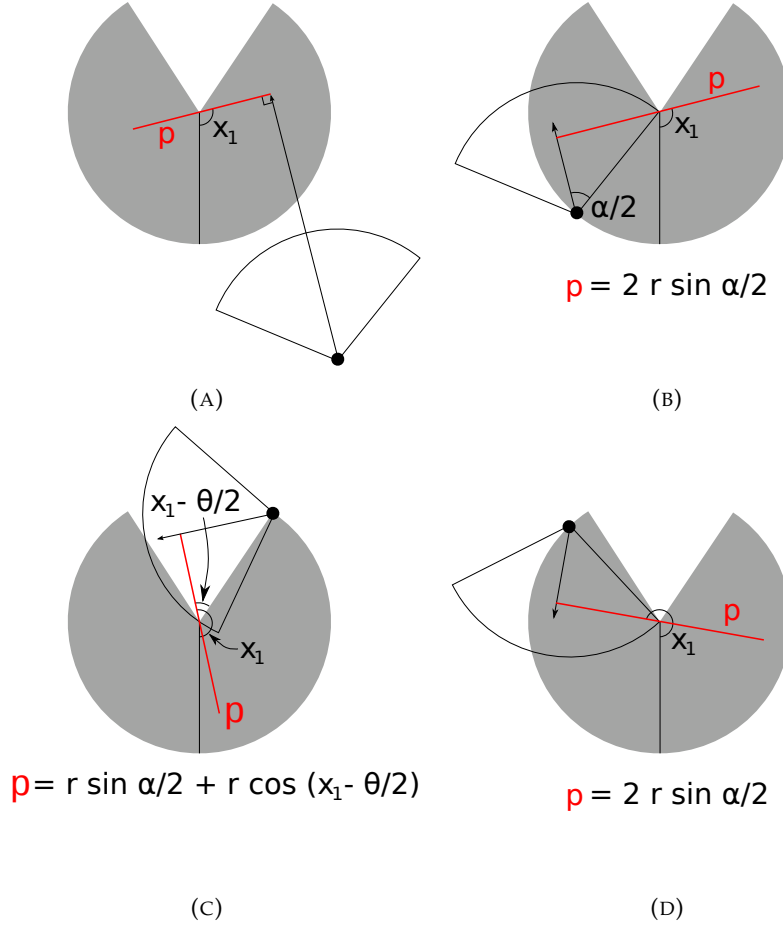


FIGURE 3. An overview of the derivation of SE2. The filled circles represent animals, with the animal signal shown as an unfilled sector and the direction of movement shown as an arrow. The detection zone of the sensors are shown as filled grey sectors with a detection distance of r . The SYMBOL shows the direction the sensor is facing; θ , sensor detection width; α , animal signal width. The profile p (the line an animal must pass through in order to be captured) is shown in red and x_1 is the focal angle, where (a) shows the location of x_1 . The derivation of p changes as the animal approaches the sensor from different directions where (b) is the derivation of p when x_1 is in the interval $[\frac{\pi}{2}, \frac{\pi}{2} + \frac{\theta}{2} - \frac{\alpha}{2}]$, (c) p when x_1 is in the interval $[\frac{\pi}{2} + \frac{\theta}{2} - \frac{\alpha}{2}, \frac{3\pi}{2} - \frac{\theta}{2} - \frac{\alpha}{2}]$ and (d) p when x_1 is in the interval $[\frac{3\pi}{2} - \frac{\theta}{2} - \frac{\alpha}{2}, \frac{3\pi}{2}]$. The resultant equation for p is shown beneath each figure.

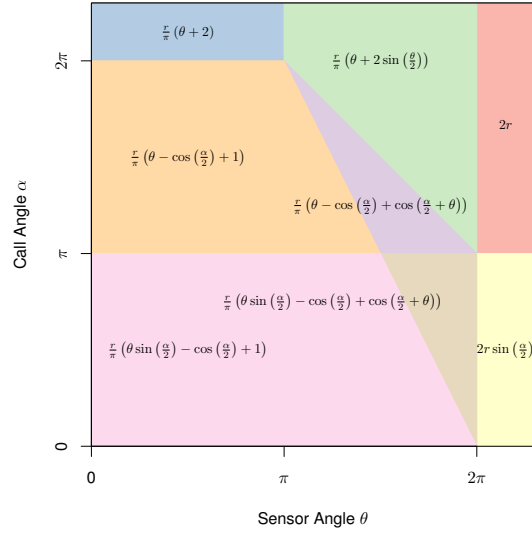


FIGURE 4. Equations for the profile wide, p , given sensor and call widths. Each colour block represents one equation, despite independent derivation within each block, many models result in the same expression. These are collected together and presented as one block of colour.

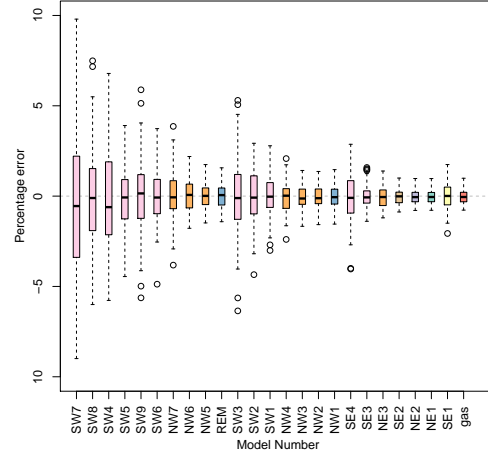


FIGURE 5. Distribution of the bias for each of the derived models. Percentage error of analytical model calculated from the simulation when settings are: $r = 100\text{ m}$; $T = 150\text{ days}$; $v = 40\text{ km days}^{-1}$; $D = 70\text{ animals km}^{-2}$; and with detection angles varying between models. The numbers referred to here can be found in Figure 1 Appendix S2, and the colour of each box plot match the functional form of the equation as seen in Figure 4.

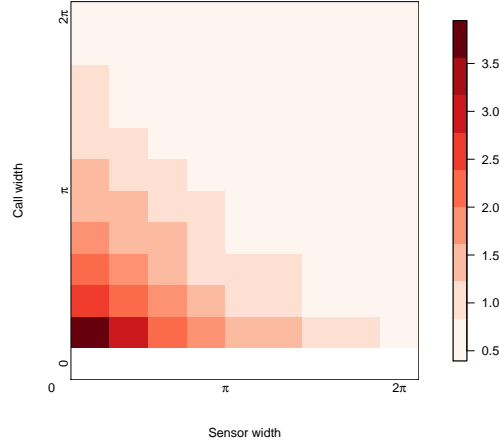


FIGURE 6. The precision of the gREM given a range of detection and call angles. The standard deviation of the percentage error for sensor, and call angles between 0 and 2π where: $r = 100$ m; $T = 150$ days; $v = 40$ km days⁻¹; $D = 70$ animals km⁻²; and with detection angles varying between models. Where red indicates a high standard deviation and blue represents a low standard deviation.

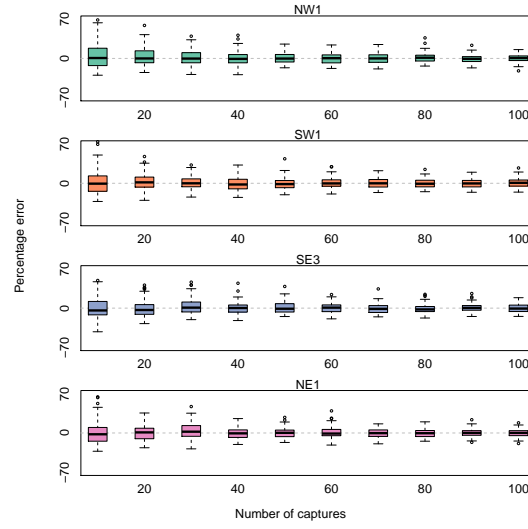


FIGURE 7. Accuracy of the gREM remains unchanged, whilst precision increases, with captures. Boxplots of four test models when given different numbers of captures where: $r = 100\text{ m}$; $T = 150\text{ days}$; $v = 40\text{ km days}^{-1}$; $D = 70\text{ animals km}^{-2}$; and with angles varying between models. Where the model names refer to Figure 1 in Appendix S2.

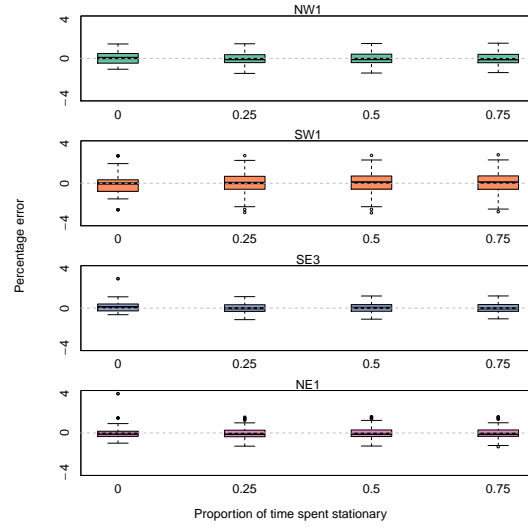


FIGURE 8. Accuracy and the precision of the gREM given changes in the amount of time an animal spends stationary on average. Distribution of model error when simulated animals spend increasing proportion of time stationary where: $r = 100$ m; $T = 150$ days; $v = 40$ km days⁻¹; $D = 70$ animals km⁻²; and with detection angles varying between models. Where the model names refer to Figure 1 in Appendix S2.

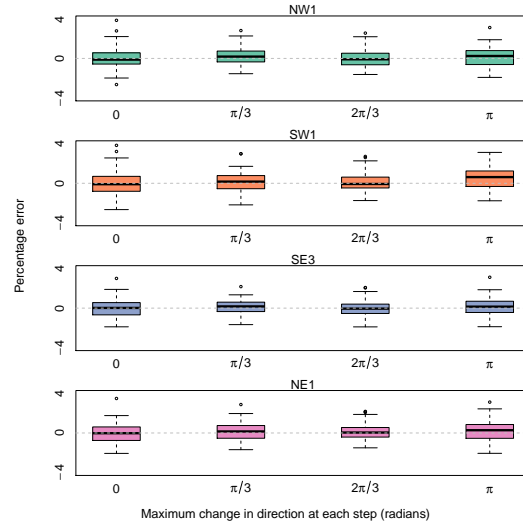


FIGURE 9. Accuracy and the precision of the gREM given different types of correlated walks. Distribution of model error when simulated animals move with different types of correlated walk where: $r = 10$ m; $T = 352$ days; $v = 40$ km days⁻¹; $D = 70$ animals km⁻²; and with angles varying between models. Where the model names refer to Figure 1 in Appendix S2.